UDC 621.383.5

RECENT PROGRESS IN AMORPHOUS SILICON SOLAR CELLS

Yoshiyuki Uchida
Hiroshi Sakai
Takeshige Ichimura
Masaharu Nishiura
Hiromu Haruki

1. INTRODUCTION

Fuji Electric Co. Ltd. has conducted intensive research and development efforts on an amprphous silicon (a-Si) solar cell and succeeded in bringing the a-Si solar cell into market as a power supply for a hand-held electronic calculator in 1980 for the first time in the world. In so far as the a-Si solar cell for a power generation is concerned, Fuji Electric has participated in the Sunshine Project since 1980 and promoted research and development on large area a-Si solar cell suitable for practical use. Since the earlier part of our work was published in this journal[1], this paper mainly describes the recent outcome and status of a-Si solar cell.

II. A-SI SOLAR CELL

1. Progress in conversion efficiency

Conversion efficiency (η) is defined as a ratio of converted electric energy to incident energy (Pin) and is written as the equation (1) using a open circuit voltage (V_{OC}), a short circuit current (Jsc) and a fill factor (FF).

$$\eta = \frac{Pm}{Pin} = \frac{Vm \times Jm}{Pin} = \frac{Voc \times Jsc \times FF}{Pin} \times 100\ (\%) \quad \ldots (1)$$

In the equation, Pm represents a maximum output power, and Vm and Jm are voltage and a current at maximum output power, respectively.

Figure 1 shows the progress in a-Si solar cell conversion efficiency since 1974 when an a-Si solar cell was reported for the first time[2]. The solid line in the figure represents the conversion efficiency of the a-Si solar cell with a small area (several mm^2) and the dotted line corresponds to that with the area of $100cm^2$, respectively. The conversion efficiency has made a remarkable progress during past few years[3].

Recently, Fuji Electric has obtained the conversion efficiency of over 7% in the $100cm^2$ area solar cell using a glass substrate and hopeful outlook realizing a-Si solar cells for power generation use[4].

2. Photovoltaic mechanism in an a-Si solar cell

The principle for converting the sunlight to electricity in a p-i-n type cell is schematically shown in *Fig. 2*.

Though not shown in the figure, a transparent conductive (TCO) film is formed on the p-layer to act as both a transparent electrode and an anti-reflection coating; in this case the cell is illuminated through the p-type window-side layer. Hole-electron pairs generated in the i-layer by the absorbed light are separated by the electric field across the

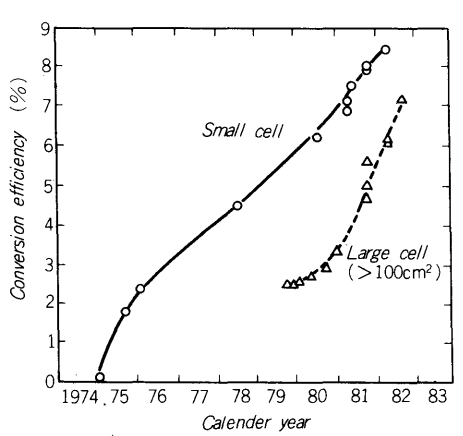

Fig. 1 Progress in the a-Si solar cell conversion efficiency

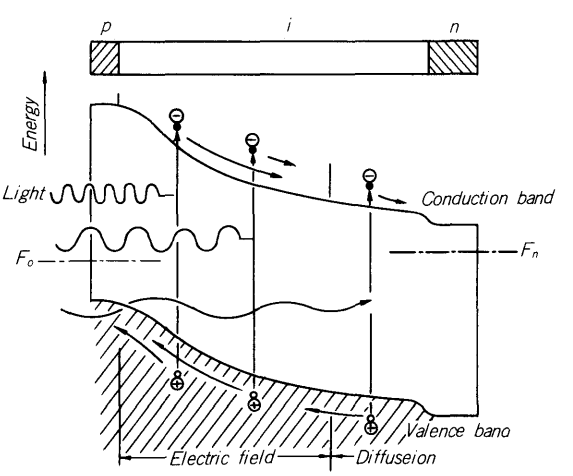

Fig. 2 Illustration of energy band profile explaining the photovoltaic mechanism in an a-Si pin junction solar cell

i-layer and an output current is generated. To increase the output current, it is effective to reduce surface reflection and absorption losses of incident light in the window-side layer and to increase the photon flux reaching the i-layer which acts as a photo-carrier generator in the cell.

Indium-Tin-Oxide (ITO) and SnO_2 are widely used as the TCO film. The thickness of the TCO film should be optimized to reduce the overall reflectance. By applying a-SiC:H or microcrystalline Si:H to the window-side layer of a cell, the output current increases considerably because of the low absorption loss in the window-side layer. The thickness of i-layer should be optimized in conjunction with drift length of carriers $\mu\tau E$ (μ: mobility, τ: lifetime, E: electric field) to obtain the maximum power output. The detailed discussion will be presented in Chapter III.

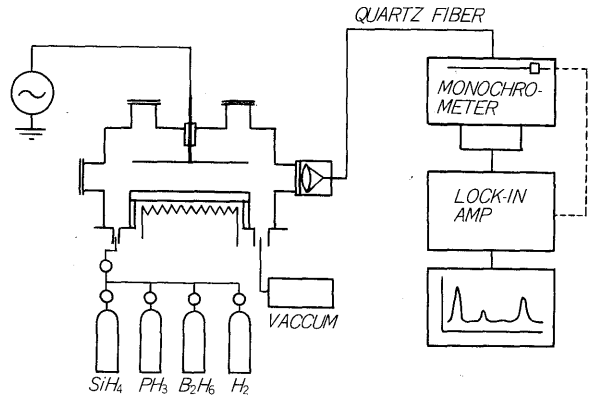

Fig. 3 Schematic of a-Si deposition system equipped with optical emmission spectroscopy (OES)

III. EXPERIMENTAL RESULTS

1. Deposition techniques of a-Si film

The a-Si for solar cell applications is a non-crystalline material called hydrogenated a-Si (a-Si:H) in which hydrogen atoms are taken into the network of Si atoms.

This material is formed by the glow discharge decomposition of SiH_4 gas and its quality depends on the plasma deposition condition such as substrate temperature, discharge power, gas pressure, flow rate and so on. *Figure 3* shows a schematic of the a-Si deposition system which is equipped with the optical emission spectroscopy (OES) for diagnosing the emissive species in plasma. The OES is a useful tool to control the plasma condition for a-Si deposition. For obtaining p-type or n-type a-Si, diborane (B_2H_6) or phoshine (PH_3) is added to SiH_4 during the deposition, respectively.

1) Microcrystalline Si:H films

A microcrystalline Si:H film in which crystal and amorphous phases coexists is formed when SiH_4 gas diluted in H_2 is decomposed by high power glow discharge[5]. Both in n and p-types of microcrystalline films, the absorption coefficient is about a half of that in the a-Si:H film. *Figure 4* shows the optical absorption spectra of the n-type films deposited with various discharging power. X-ray diffraction measurements showed that the film deposited with a discharging power of 20W had no crystalline pahse and the crystallization was enhanced with increasing discharging power.

Figure 5 shows the dark conductivity as a function of discharging power for the film deposition, along with the activation energy of the conductivity. By increasing the discharging power, the conductivity increases drastically from 10^{-4} to 8 $(ohm\ cm)^{-1}$, and the activation energy changes from 0.2 eV to 0.02 eV, correspondingly. We have also ascertained that microcrystallization occurs even in a very thin (100 Å) Si:H film[6].

2) A-SiC:H film

A-SiC:H film is formed by the glow discharge of SiH_4 – CH_4 gas mixture. *Figure 6* shows the absorption coefficient of a film formed by decomposing (1-x) SiH_4 + x

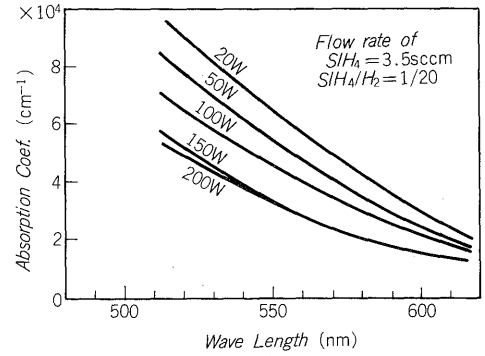

Fig. 4 Absorption spectra of the films deposited with various discharging power

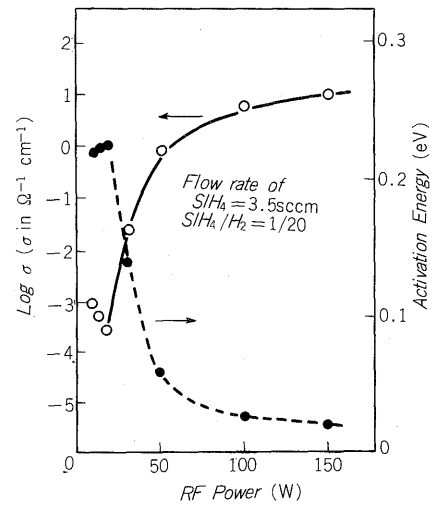

Fig. 5 Conductivity at room temperature and activation energy vs. discharging power for P-doped Si:H films

CH_4 gas mixture as a function of gas fraction x. With increasing CH_4 content, the absorption coefficient decreases and that at the wavelength of 550 nm is 1.1×10^4 cm^{-1} when x is 0.7, while it is 5.7×10^4 cm^{-1} for the a-Si:H film.

The characteristics of boron doped a-SiC:H film (x=0.7) is shown in *Fig. 7*. The optical bandgap of the film

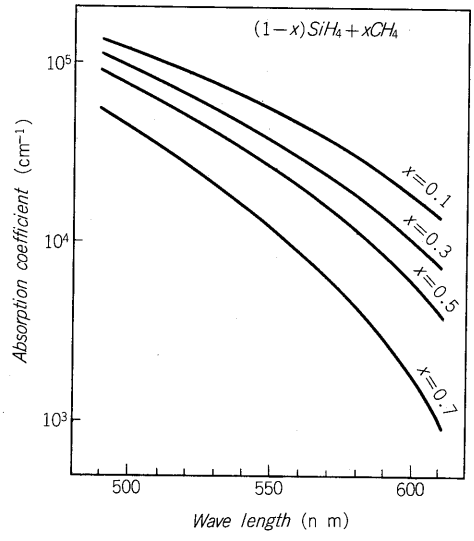

Fig. 6 The absorption coefficient of a-SiC:H film as a function of wavelength with a parameter of gas fraction x

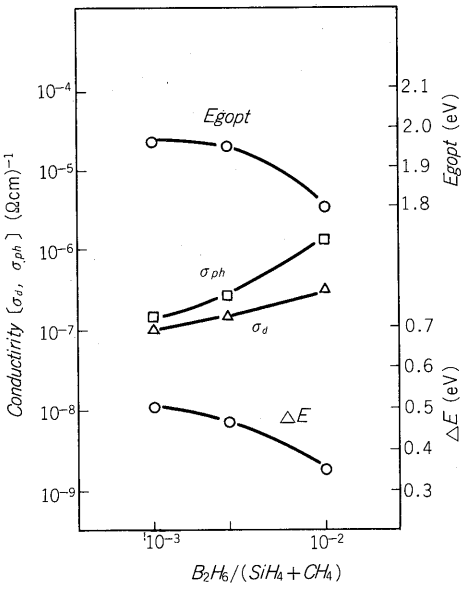

Fig. 7 The characteristics of boron-doped a-SiC:H film versus boron density

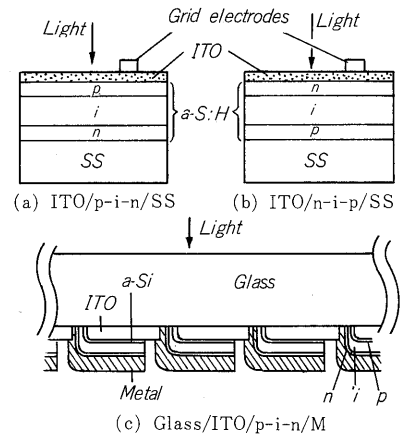

Fig. 8 Schematic structures of a-Si solar cells

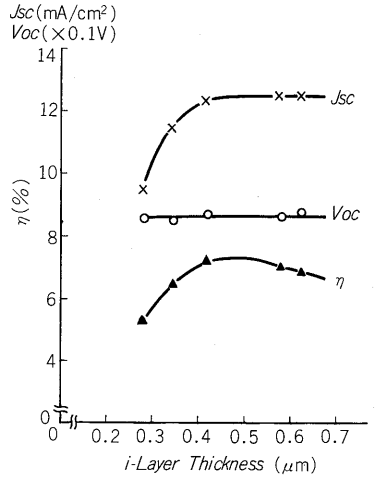

Fig. 9 Dependence of characteristics in the ITO/n-i-p/ss cell on i-layer thickness

is over 1.9 eV when doron is doped with the gas ximture whose composition $B_2H_6/(SiH_4 + CH_4)$ is 0.003. This suggests that the boron doped a-SiC:H film is promising for the window layer of the a-Si solar cell.

2. Structures and characteristics of a-Si solar cell

1) Structures of a-Si solar cells for the power generation

Figure 8 shows schematic structures of a-Si solar cells studied so far in Fuji Electric. Since the a-Si film consists of p-, i- and n-type leyers, the solar cells are called a p-i-n type a-Si solar cell. The a-Si solar cell formed on a stainless steel (ss) substrate possesses ITO/p-i-n/ss and ITO/n-i-p/ss structures. In ITO/p-i-n/ss structure, the p-layer works as the window-side layer [(a): forward type cell], while in ITO/n-i-p/ss structure, the n-layer works as the window-side layer [(b): inverted type cell]. In the a-Si solar cell formed on a glass substrate, light enters the cell through the glass substrate and electrically isolated p-i-n cells are connected in series [(c)].

It is important to optimize the thikness of a window-side layer in the forward and the inverted type cells as well as the thickness of an i-type a-Si layer in the p-i-n type cell. *Figure 9* shows output characteristics as a function of i-layer thickness in the inverted type cells. The Jsc increases with the i-layer thickness. This is due to the increses of photons absorbed in the i-layer which generate photo-carriers. However, when the thickness of i-layer becomes too thick, a part of i-type a-Si film acts as a series resistance against the current flow, which causes the degradation of *FF* and the conversion efficiency. It has been found that the conversion efficiency reaches maximum when the i-layer is 0.4 to 0.5 μm in thickness.

We found that boron atoms are taken in the i-type a-Si layer of the inverted type cell as shown in *Fig. 10* and the boron concentration has a great effect on a cell characteris-

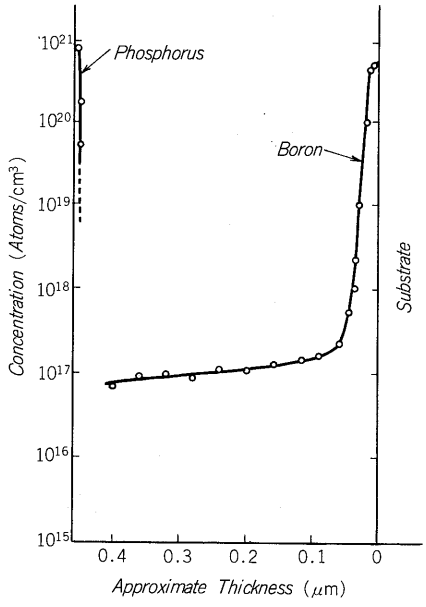

Fig. 10 Dopant profile in the n-i-p a-Si:H layers

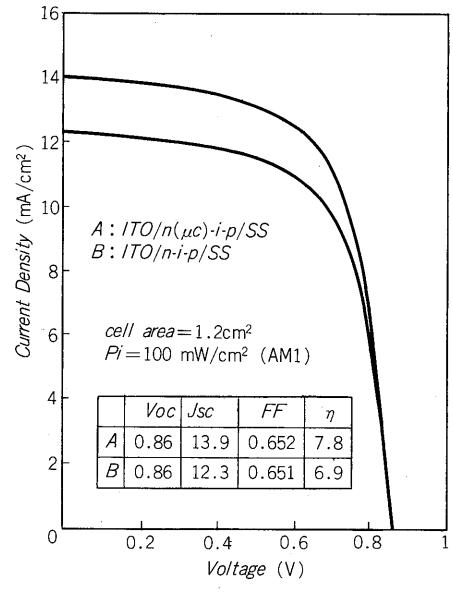

	Voc	Jsc	FF	η
A	0.86	13.9	0.652	7.8
B	0.86	12.3	0.651	6.9

Fig. 11 The cell characteristics of ITO/n(μc)-i-p/ss and ITO/n-i-p/ss cells

tics[7]. The maximum conversion efficiency can be obtained when about 1×10^{17} atoms/cc of boron atoms exists in the i-type a-Si layer. In such an i-type a-Si layer the Fermi level lies at the center of its band gap. Our experimental studies suggest that by low level boron doping the drift length of photogenerated holes in the i-layer becomes longer than that in non-doped i-layer.

2) Application of microcystalline Si:H film to solar cells

As the absorption coefficient of microcrystalline Si:H film is lower than that of a-Si:H film as mentioned in the previous section, the conversion efficiency can be expected to increase when this film is applied to the window-side layer of a p-i-n type solar cell. *Figure 11* shows the output characteristics of the inverted type cells to which an n-type microcrystalline Si:H film is applied as a window-side layer. As is known from the figure, Jsc is improved in the new type cell compared with that in the inverted cell having conventional amorphous and conversion efficiency of 7.8% has been obtained[9].

3. Large area a-Si-solar cells

1) Stainless steel (ss) substrate cells

Conversion efficiency of the a-Si solar cell depends on the cell area; conversion efficiency decreases with increasing cell area. The conversion efficiency reduction is mainly related to the decrease of *FF* and J_{SC} with the enlargement of cell area[10]. We analyzed the cause of the reduction in *FF* and J_{SC} by examining the power loss due to grid electrodes, contact resistances and so on.

We found that the reduction of *FF* and J_{SC} associated with increasing the cell area from 1.2 cm² to 100 cm² is caused by the factors shown in *Table 1*[4]. Almost half the decrease in *FF* is caused by power loss due to series resistance. The power loss caused by the current flow along the stem part of grid electrodes shown in *Fig. 12 (a)* occupies the most part of the power loss due to series resistance. We designed and prepared other two types of 100 cm² cells shown in *Fig. 12 (b)* and *(c)* aiming at reducing power loss in the stem part of the grid electrode. In these cells, the photocurrent is collected without flowing along the direction of the longer side of the stem, and thus the series resistance in the stem part of grid electrodes can be neglected. As a result the conversion efficiency of more than 6% was obtained in 10×10 cm² (b) and 5×20 cm² (c) solar cells. Both cells show the same *FF* of 0.60 while that of the cell shown in *Fig. 12 (a)* is about 0.55.

2) Glass substrate cells

For the glass substrate cell shown in *Fig. 8 (c)*, we calculated the total output photovoltaic power as a function of unit cells connected in series by considering the power losses in the ITO and metal electrodes. The results are shown in *Fig. 13*. The $1_2 + 1_3$ in the figure represents the connection length between unit cells. The calculation shows that the maximum output power is obtained in the 100 cm² glass substrate cell when about 10 cells are con-

Table 1 Factors influencing the cell area dependence of JSC and FF (1.2 cm² and 100 cm² cells)

Cell area	FF	J_{SC} (mA/cm²)
1.2 cm²	0.659	11.2
100 cm²	0.549	10.6
Difference	0.110	0.6
Contribution to FF & Jsc lowering		
Shunt resistance	10%	
Series resistance	50%	
Inhomogeneity	10%	100%
Contact resistance	30%	

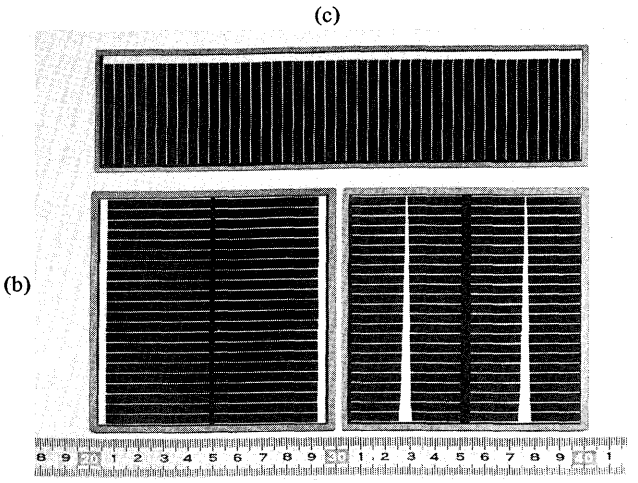

Fig. 12 Three types of ss-substrate cells with 100 cm² area

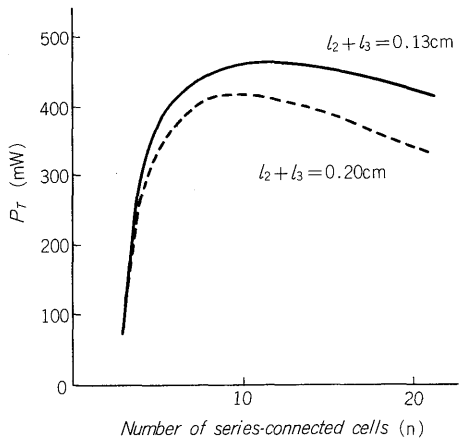

Fig. 13 Output photovoltaic power as a function of the number of series-connected unit cells in the glass-substrate cell

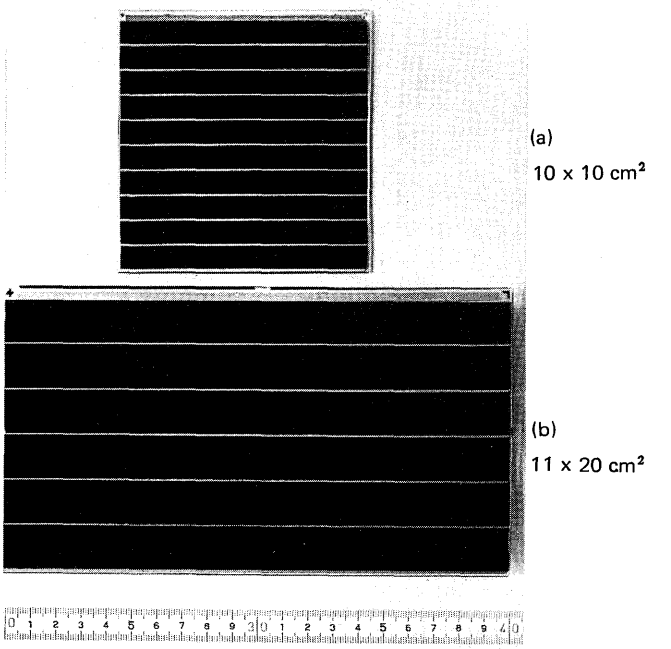

Fig. 14 Glass-substrate cells

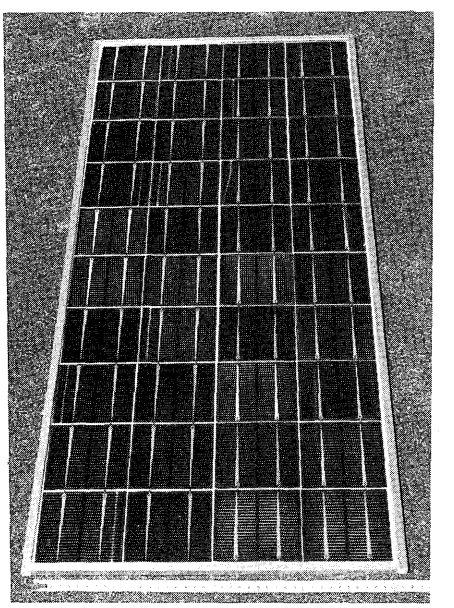

Fig. 15 a-Si photovoltaic module with superstrate structure composed of 40 cells of 10 x 10 cm in area

nected in series under the condition that ITO sheet resistance is 10 Ω/□.

Figure 14 shows two types of a-Si solar cells formed on a glass substrate. In *Fig. 14 (a)* 10 cells are connected in series (10 x 10 cm²) and in *Fig. 14 (b)* 6 cells are connected in the same way (11 x 20 cm²).

The conversion efficiency of over 7% was obtained in the former cell (a) using the a-SiC:H layer having a superior transmittance at the side of incident light. In a 11 x 20 cm² cell the conversion efficiency of 6.0% was obtained[4].

4. The a-Si photovoltaic module

The a-Si photovoltaic cells can be formed on several kinds of substrates such as metal, glass and polymer film. Optimum module structure depends on the substrate materials.

For ss-substrate cells we adopt the superstrate structure. Semi-tempered sodalime glass plate, silicone resin and polyvinyl fluoride (PVF) film are used for a front cover, encapsulant and a back cover, respectively. *Figure 15* shows the module composed of 40 cells each 10 x 10 cm² in area. These 40 cells are wired in 4 parallel strings of 10 cells wired in series.

The electric output power under AM1 (100 mW/cm²) illumination lies between 15 W and 20 W.

There is another possibility to make a low cost module with a glass substrate cell. The substrate glass plate can be used for front cover of the module as shown in *Fig. 8 (c)*. In this case, an a-Si photovoltaic module can be constructed on a single large area glass plate. As a first step of investigat-

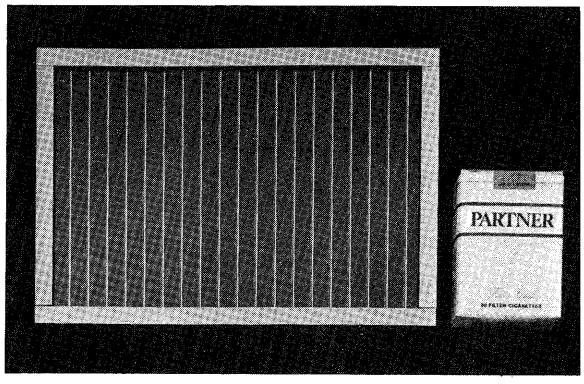

Fig. 16 Single substrate module

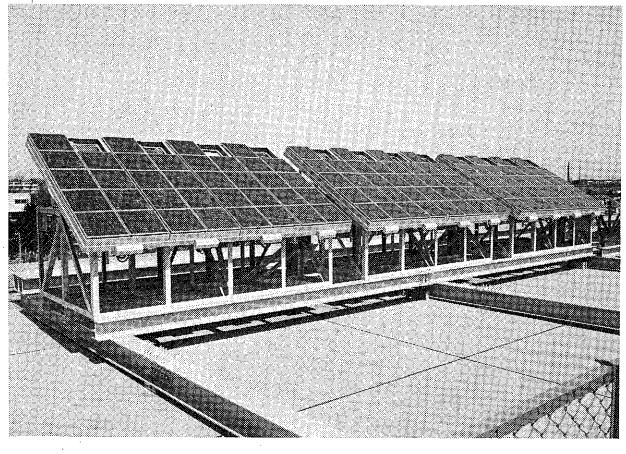

Fig. 17 a-Si solar cell array

ing "single substrate module", we made a module with a large area glass substrate cell of 15 x 22 cm^2 as shown in *Fig. 16*.

IV APPLICATION OF A-SI SOLAR CELL

1. For photovoltaic power generation

We have made some photovoltaic systems with a-Si modules for experimental purposes.

Figure 17 shows a solar cell array which consists of 108 pieces of the a-Si module composed of 36 sheets of 49 cm^2 solar cells made by Fuji Electric[1]. This solar cell array has an about 400 W power generating ability under AM1. It was installed as a joint work between The Tokyo Electric Power Co. Inc. and Fuji Electric in the spring of 1981, and is now under field test to evaluate system reliability.

Clocks on the advertisement tower of Fuji Electric in Tokyo and at the museum of Ohmachi (*Fig. 18*) were implemented by a-Si solar arrays equipped with a storage system.

2. For consumer electronics

Fuji Electric has already brought many a-Si solar cells for consumer goods such as electronic calculators, clocks

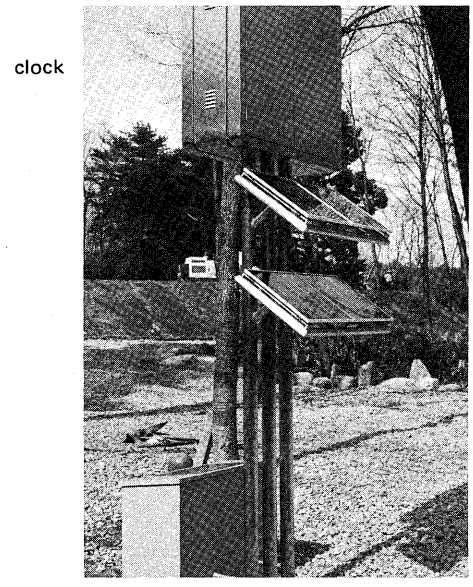

Fig. 18 A clock powered by the a-Si solar cell at the museum of Ohmachi

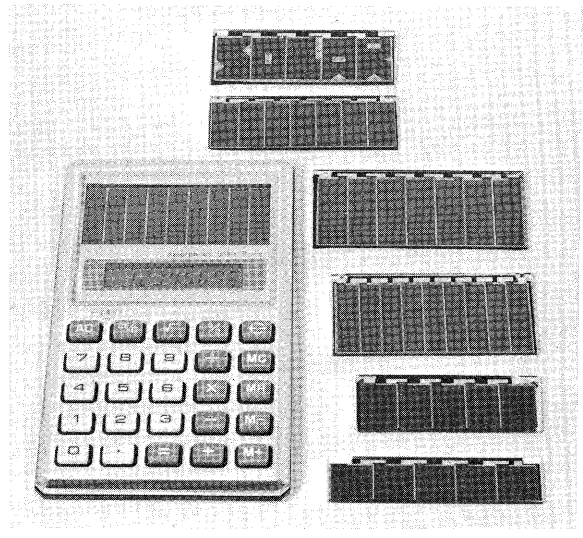

Fig. 19 a-Si solar cells for calculator

and watches into market. In a clock or a watch the a-Si solar cell is used together with a power source such as a silver oxide battery to extend service life of the battery, while the a-Si solar cell drives an electronic calculator under the room light of less than 200 lux without any battery storage system.

Figure 19 shows a-Si solar cells for electronic calculator presently in the market. Since the a-Si solar cell has been successfully applied to an electronic calculator, it will find many other applications in the near future.

V. SUMMARY

Recent developments on a-Si solar cells in Fuji Electric have been reviewed. Here we summarized the significant

results:

(1) The highest conversion efficiency for the ITO/n-i-p/ss cell is obtained when the concentration of boron incorporated in the i-layer is around 1×10^{17} atoms/cm^3.
(2) The microcrystalline phosphorus-doped Si:H and the boron-doped a-SiC:H are effective materials for the window-side layer to improve the cell performance because of their low absorption coefficient.
(3) The design parameters for large-area cells have been further optimized, and the efficiency of the 100 cm^2 cell has exceeded 7%.
(4) The a-Si photovoltaic module with superstrate structure has been demonstrated.
(5) Some solar array systems have been demonstrated and many a-Si solar cells are supplied to the market for a consumer electronics.

VI. ACKNOWLEDGEMENT

The authors are greatful to Prof. Y. Hamakawa of Qsaka University for his helpful discussions. They are also greatful to Dr. A. Shimazaki and Dr. S. Fushimi for their helpful advice and enconragement.

This work was partly supported by the Agency of Industrial Science and Technology under the contract of the Sunshine Project.

References

(1) Y. Uchida et al., Fuji Electric Rev., 27 (2) (1981) 34
(2) D. E. Carlson and C. R. Wronski, Appl. Phys. Lett., 28 (1976) 671
(3) Y. Tawada et al., Solar Energy Material, 6 (1982) 299
(4) Y. Uchida et al., Proc. 161st Electrochem. Soc. Meeting, Montreal (1982) (to be published)
(5) Y. Uchida et al., J. Phys. (Paris) 42 (1981) Suppl. 10, C4-265
(6) A. Matsuda et al., J. J. Appl. Phys., 20 (1981) L439
(7) H. Haruki et al., J. J. Appl. Phys., 21 (1982) Suppl. 22-1, 283
(8) H. Haruki et al., (to be published)
(9) Y. Uchida et al., J. J. Appl. Phys. (to be published)
(10) Y. Uchida et al., Proc. 8th Intern. Vacuum Congress, Cannes, Vol. 1 (1980) 699